Three-dimensional modeling of controlled-source electromagnetic response for inductive and galvanic components

SeyedMasoud Ansari and Colin G. Farquharson
Memorial University of Newfoundland, St. John's, Canada

SUMMARY

A finite-element solution to the three-dimensional electromagnetic forward modeling problem in the frequency domain is presented. The method is based on decomposing the electric field into vector and scalar potentials in the Helmholtz equation and in the equation of conservation of charge. The problem is formulated for total fields and discretized using unstructured tetrahedral meshes. The E-field equation is firstly solved:

$$\nabla \times \nabla \times \mathbf{E} + i\omega\mu_0\sigma\mathbf{E} = -i\omega\mu_0\mathbf{J^s}$$

Decomposing the electric field into vector and scalar potentials in the above equation and equation of conservation of charge gives,

$$\nabla \times \nabla \times \mathbf{A} + i\omega\mu_0\sigma\mathbf{A} + \mu_0\sigma\nabla\phi = \mu_0\mathbf{J^s},\ -i\omega\nabla\cdot(\sigma\mathbf{A}) - \nabla\cdot(\sigma\nabla\phi) = -\nabla\cdot\mathbf{J^s}$$

The above system is solved using the finite-element method.

DISCRETIZATION

Scalar basis functions (nodal-elements) and vector basis functions (edge-elements) are used for the scalar and vector potentials respectively.

$$\mathbf{E} = -i\omega\mathbf{A} - \nabla\phi$$

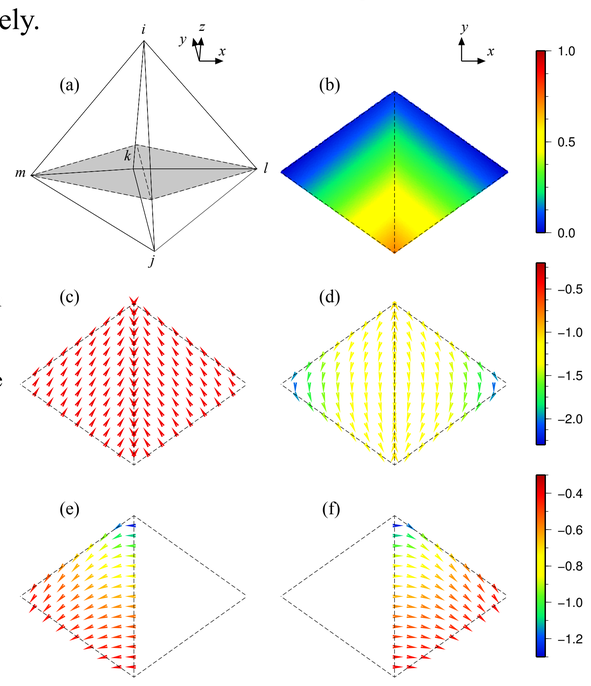

Figure 1. Scalar and vector plots for the basis functions for two identical neighbors: left (i, j, k, m) and right (i, j, k, l) cells. The plots are for the gray-shaded plane shown in panel (a). Panel (b) is the scalar basis function for the j^{th} node and panel (c) is its corresponding ∇N_j. Panel (d) shows the projection of $\mathbf{N}_{ji}$ on the gray plane for the two cells. Panel (e) and (f) respectively show the projection of the vector basis functions $\mathbf{N}_{jm}$ and $\mathbf{N}_{jl}$ on the gray plane.

Efficiency of the method: Magnetic dipole and a homogeneous half-space

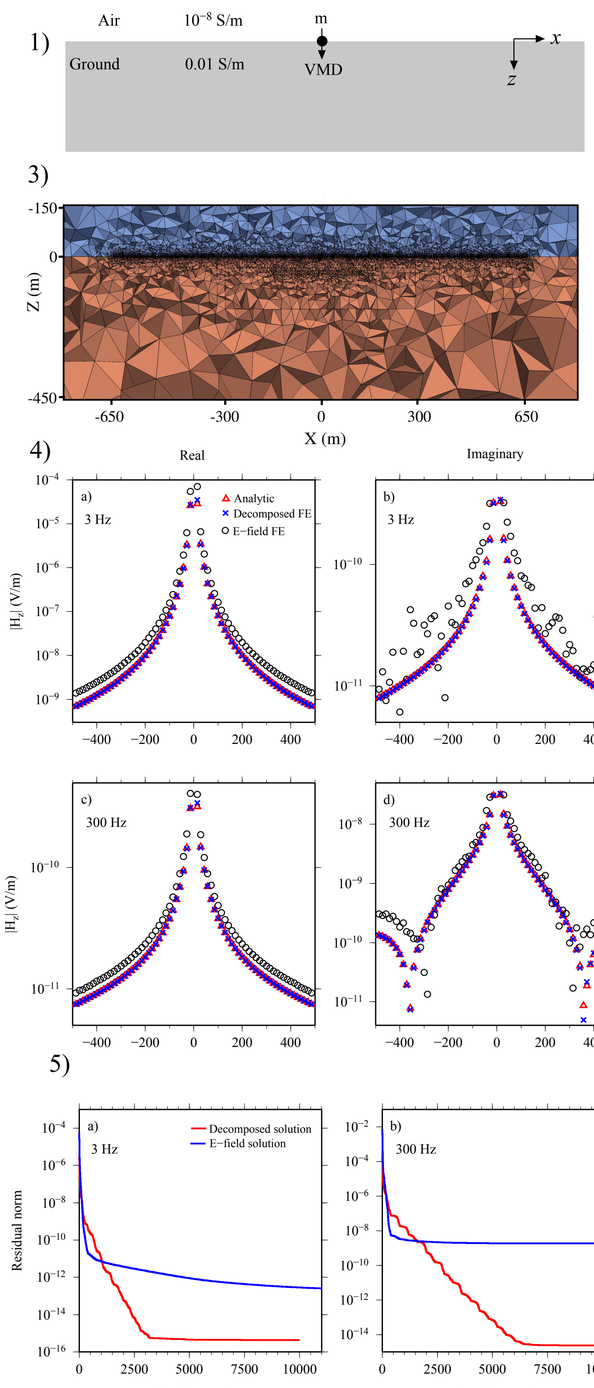

Figure 2. 1) The geometry of the homogeneous half-space. A small electric dipole source is located on the ground-air interface. 2) The entire view and 3) the enlarged cross-section of the central part of the the tetrahedral mesh. 4) A comparison of the z-components of the real and imaginary parts of the magnetic field observed on the Earth's surface. Results form the FE solution are in good agreement with the results from the analytic formula of Ward and Hohmann (1988). The solution of the E-field equation does not match the analytic data. 5) The convergence curves for the E-field and decomposed solutions for frequencies of 3 Hz and 300 Hz. 6) The inductive part (a and b), galvanic part (c and d) and total electric field (e and f) for a frequency of 3 Hz.

E-field

$$\begin{pmatrix} \mathbf{C} & -\omega\mu_0\mathbf{D} \\ \omega\mu_0\mathbf{D} & \mathbf{C} \end{pmatrix} \begin{pmatrix} \tilde{E}^R \\ \tilde{E}^I \end{pmatrix} = \begin{pmatrix} 0 \\ -\omega\mu_0 S_1 \end{pmatrix}$$

$\mathbf{A} - \phi$

$$\begin{pmatrix} \mathbf{C} + i\omega\mu_0\mathbf{D} & \mu_0\mathbf{F} \\ i\omega\mathbf{G} & \mathbf{H} \end{pmatrix} \begin{pmatrix} \tilde{A} \\ \tilde{\phi} \end{pmatrix} = \begin{pmatrix} \mu_0 S_1 \\ S_2 \end{pmatrix}$$

A generalized minimum residual solver (GMRES) with an incomplete LU preconditioner (ILUt) from SPARSKIT (saad, 1990)is used to iteratively solve the above systems.

Galvanic Effect: Grounded wire and prism in a half-space

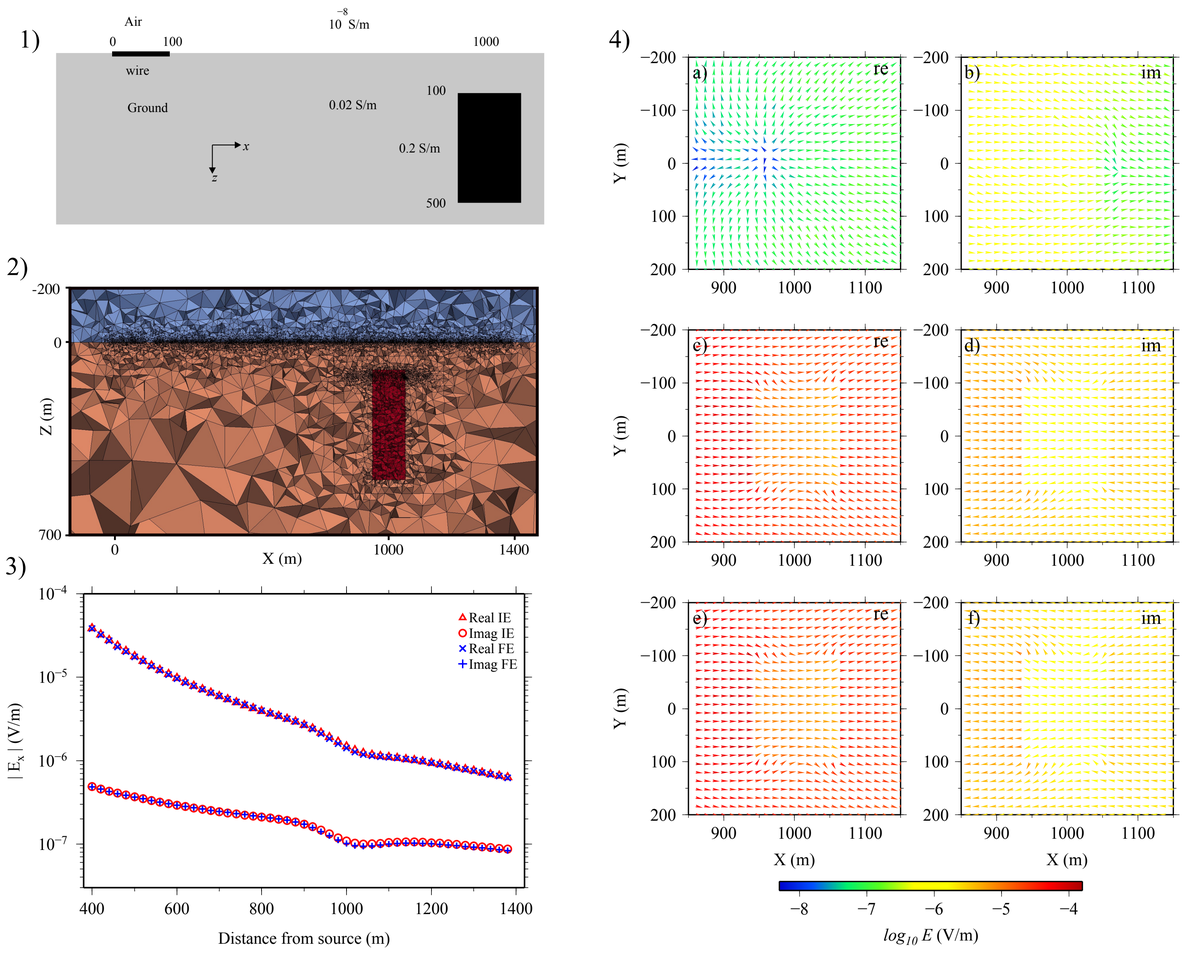

Figure 4. 1) The geometry for the prism and electric line source example. The 100 m grounded wire source is located on the air-ground interface. 2) The enlarged cross-section of the central part of the the tetrahedral mesh. 3) A comparison of the x-components of the real and imaginary parts of the electric field from the FE approach with the integral equation approach of Farquharson and Oldenburg (2002). 4) The inductive part (a and b), galvanic part (c and d) and total electric field (e and f) for a frequency of 3 Hz.

Inductive Effect: Loop-loop array for a large conductivity contrast

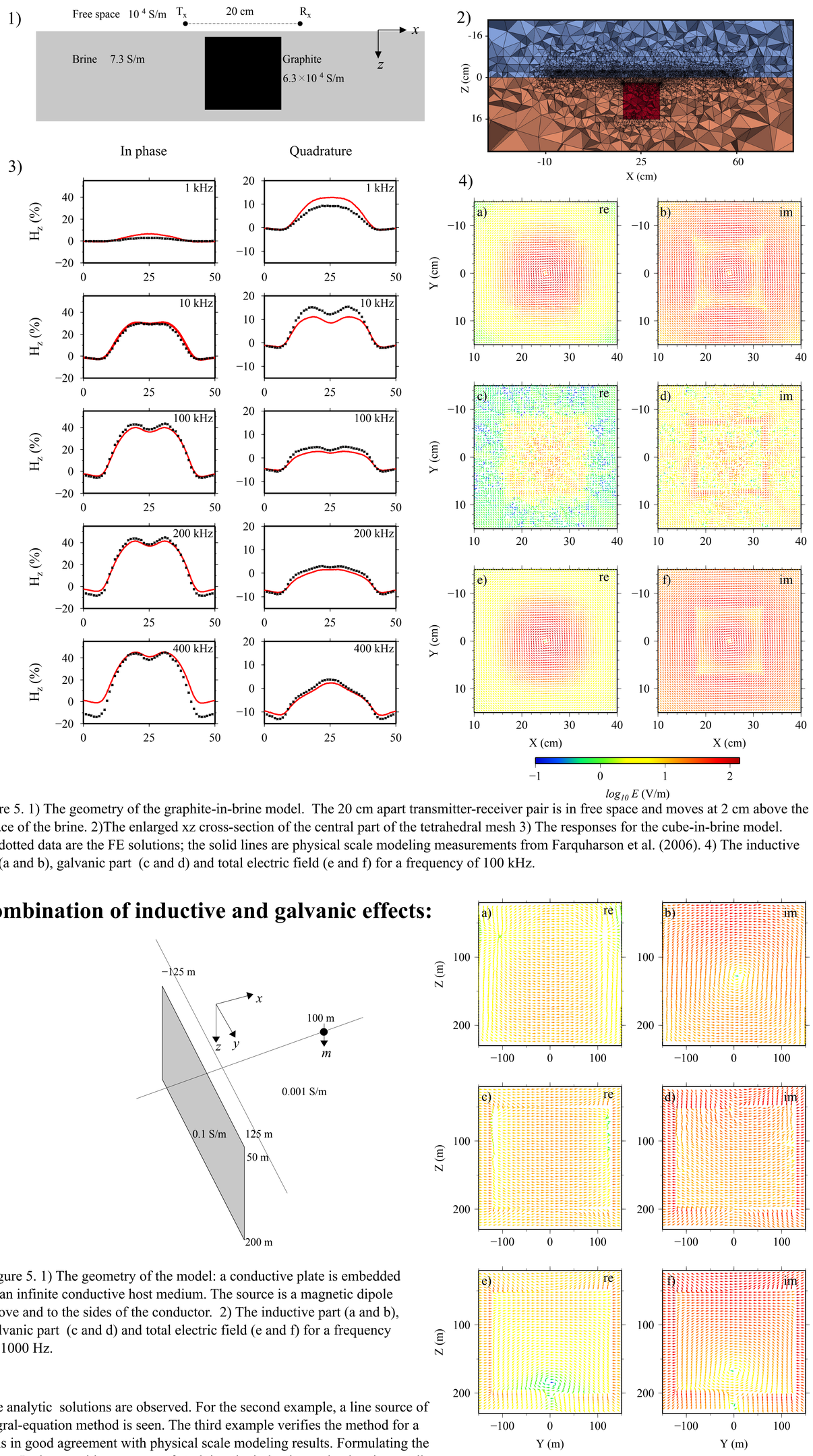

Figure 5. 1) The geometry of the graphite-in-brine model. The 20 cm apart transmitter-receiver pair is in free space and moves at 2 cm above the surface of the brine. 2)The enlarged xz cross-section of the central part of the tetrahedral mesh 3) The responses for the cube-in-brine model. The dotted data are the FE solutions; the solid lines are physical scale modeling measurements from Farquharson et al. (2006). 4) The inductive part (a and b), galvanic part (c and d) and total electric field (e and f) for a frequency of 100 kHz.

Combination of inductive and galvanic effects:

Figure 5. 1) The geometry of the model: a conductive plate is embedded in an infinite conductive host medium. The source is a magnetic dipole above and to the sides of the conductor. 2) The inductive part (a and b), galvanic part (c and d) and total electric field (e and f) for a frequency of 1000 Hz.

CONCLUSIONS

In the first example where a magnetic dipole is used a good agreement between the results from the FE approach presented in this study and the analytic solutions are observed. For the second example, a line source of current excites a relatively conductive prism buried in a half-space model. A good match between the results form the FE approach and an integral-equation method is seen. The third example verifies the method for a large conductivity contrast where a transmitter-receiver pair moves over a graphite cube submerged in brine. The FE solution for this example is in good agreement with physical scale modeling results. Formulating the problem via the decomposed fields gives, as anticipated, a significantly improved convergence of the iterative solution of the system of equations. It also provides a means of studying the inductive and galvanic contributions to geophysical EM responses. For the prism and line of curren example the galvanic component dominates the inductive component for the frequency used. For the graphite-in-brine example however, the inductive part is dominant in reducing the electric field in the medium. In the last example presented here the total EM response consists of a combination of the inductive and galvanic components.

References:

Farquharson C. G. and D. W. Oldenburg, 2002, An integral equation solution to the geophysical electromagnetic forward-modelling roblems, in M. S. Zhdanov and P. E. Wannamaker, eds., Three-Dimensional Electromagnetics: Elsevier, Inc., 3-19.

Farquharson, C. G., K. Duckworth, and D. W. Oldenburg, 2006, Comparsion of integral equation and physical scale modeling of the electromagnetic response of models with large conductivity contrasts: Geophysics, 71, G169–G177.

Lajoie J. J. and G. G. West, 1976, The electromagnetic response of a conductive inhomogeneity in a layered Earth, Geophysics, 41, 1133-1156

Ward S. H. and G. W. Hohmann, 1988, Electromagnetic Theory for Geophysical Applications, in M. N. Nabighian, eds., Electromagnetic Methods in Applied Geophysics: Society of Exploration Geophysicists,1, 131-311.

Saad, Y., 1990, Sparskit: A basic tool kit for sparse matrix calculations, report RIACS-90-20: Research institute for advanced computer science, NASA, AMES research center.

Contacts:

SeyedMasoud Ansari seyedmasoud.ansari@mun.ca
Colin G. Farquharson cgfarquh@mun.ca